Optical properties of Co^{2+} substituted $BaFe_{12}O_{19}$ hexaferrite nanoparticles via sol-gel auto-combustion route

Varsha C. Chavan[1], Maheshkumar L. Mane[2]*, U. B. Dindore[3], S. E. Shirsath[4], A. B. Ghumare[2], Surendra S. More[1]

[1]Department of Physics, Yashawantrao Chavan Mahavidyalaya, Tuljapur, MS, India,
[2]Department of Physics, S. G. R. G. Shinde Mahavidyalaya, Paranda, MS, India,
[3]Department of Physics, Adarsh College, Omerga, Dist. Osmanabad, MS, India,
[4]Department of Physics, Vivekananda Mahavidyalaya Aurangabad, MS, India.

Abstract

This paper presents investigations on structural, optical, magnetic and dielectric properties of technologically important Co^{2+} substituted $BaFe_{12}O_{19}$ ferrite nanoparticles prepared by sol-gel auto-combustion technique. The structural properties were investigated by using X-ray diffraction technique. Diffuse Ray spectroscopy technique for optical data measurement is discussed. The compositional dependence of the electrical properties of the substituted barium hexaferrite was investigated by DC electrical resistivity and Dielectric measurements. The dielectric behavior obeys the Maxwell-Wagner polarization in accordance with Koops phenomenological theory. The good electric resistivity associated with high dielectric constant and dielectric loss qualifies the ceramics for high frequency applications.

Keywords: Barium hexaferrite; DC electrical resistivity; Dielectric properties.

1 Introduction

Electromagnetic wave absorbers are becoming quite indispensable to preventing the electromagnetic pollution of the environment. There are two kinds of magnetic absorbers, including magnetic metal materials and ferrite materials, have been developed for the MHz to GHz frequency range microwave absorbers. In the development of ferrite-based microwave absorbers, the spinel ferrites have been most widely utilized as microwave absorbing materials. But it is difficult to use at frequency over 2GHz due to Snoek's limit [1–3]. Compared to spinel ferrites with a cubic crystallographic structure, the hexagonal ferrites with a magnetoplumbite structure, have a higher resonance frequency and higher microwave permeability, and therefore are more useful in the higher frequency range [4]. Since $BaFe_{12}O_{19}$ (BaM) has a natural ferrimagnetic resonance around several 10GHz due to the high magnetic anisotropy field [5]; the reduction of

the magnetic anisotropy by the substitution of Fe^{3+} produces the ferrimagnetic resonance at the lower microwave frequency range. S. Sugimoto et al. reported the reduction of the natural resonance frequency by the substitution of Fe^{3+} in M-type barium hexaferrite [6]. The substitution of other ions for some Fe^{3+} ions is also an effective method to vary the magnetic properties and electrical properties of ferrites.

A variety of different cation substitutions are possible in $BaFe_{12}O_{19}$. Divalent transition metals such as $Ni^{2+/3+}$ and $Co^{2+/3+}$ for $Fe^{2+/3+}$ are frequently used due to their similarity in ionic radii and electronic configurations. However, both the electrical and magnetic properties of substituted BaM ferrites are strongly dependent on the synthesis conditions as disproportionate charge distributions generally occur for multivalent cationic doping. There is also a concomitant structural implication when doping with $Co^{2+/3+}$ ions influencing the magneto-dielectric properties of this compound. Thus, cobalt doping in particular has been the subject of many such investigations [7-9]. The Co^{2+} mainly enter the octahedral $4f_2$ sites giving a negative contribution to the anisotropy constant K_1. In other words, the substitution of Co^{2+} cations is effective to decrease the resonance frequency down to the microwave range by reducing the magnetic anisotropy field. Therefore Co^{2+} substituted BaM could find application in perpendicular recording due to their excellent high frequency response. In this study the effect of Co^{2+} substitution in place of Ba^{2+} prepared by sol-gel auto-combustion technique for their optical and electrical properties has been discussed in details.

2 Experimental Techniques

Stoichiometric Co^{2+} substituted $Ba_{1-x}Co_xFe_{12}O_{19}$ (x = 0.0 to 1.00 with steps of 0.25) ferrite nanoparticles were prepared by sol-gel auto-combustion technique using AR grade nitrates of respective cations $Ba(NO_3)_2 \bullet 6H_2O$, $Co(NO_3)_2 \bullet 6H_2O$, $Fe(NO_3)_3 \bullet 9H_2O$. Citric acid was used as chelating agent. All starting materials were dissolved in de-ionized water with required molarities. The metal nitrate to citric acid ratio was mentioned at 1:3. The solutions of the precursors were mixed and heated on hot plate with violent stirring. The pH of the solution plays a major role in the formation of a compound. The pH of the solution was kept at 8 by using ammonia solution. This final solution was consciously stirred to get fine particle size with greater homogeneity. The obtained fine particles were sintered at 600 ^oC for 6 hrs and used as precursor for further characterizations.

The standard power X-ray diffraction technique in the region of 2θ = 20–80 with a step scan of 0.02^o/min on a Philips diffractometer (Model PW1710) using CuKα radiation (λ=1.5406 Å) is employed to

determined the crystal structure and phase purity of the samples. The UV–Visible diffuse reflectance spectrum (DRS) was recorded to estimate their band gap energy. The DC resistivity of the samples was measured using the two-probe method in which silver paste was used as a contact material. The samples were firmly fixed between two electrodes to produce good surface contact. An auxiliary heater was used for heating all of the investigated samples. The temperature was measured using a chromel–alumel thermocouple from room temperature to beyond Curie temperature with the steps of 10K. The frequency dependence of dielectric constant (ε′) and dielectric loss tangent (tanδ) were studied using a precision LCR meter bridge (Model HP 4284 A).

3 Results and discussion

3.1 X-ray diffraction technique

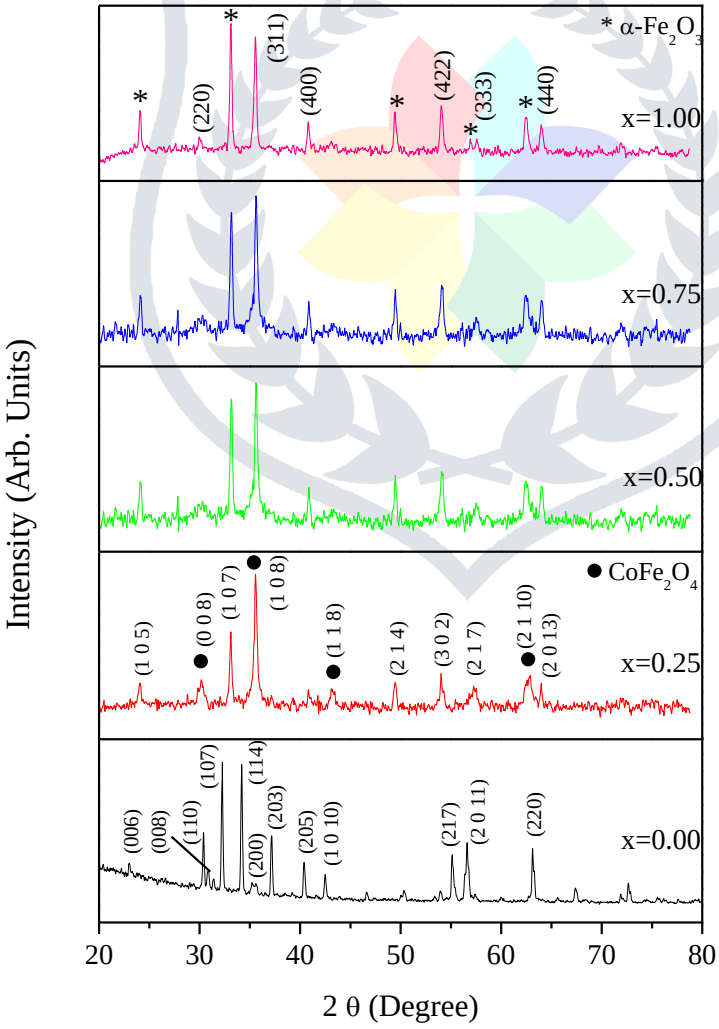

Fig. 1: X-ray diffraction patterns of $Ba_{1-x}Co_xFe_{12}O_{19}$

The X-ray diffraction pattern for all the samples of $Ba_{1-x}Co_xFe_{12}O_{19}$ (x= 0.0 to 1.00) is shown in Figure 1. For all the supposed samples crystal structure was confirmed, i. e. for pure $BaFe_{12}O_{19}$ sample crystal structure is single phase hexagonal ferrite, while for x = 0.25 to 1 the crystal structure shows phases of hexagonal as well as spinel ferrite. However, a small trace of residual α-Fe_2O_3, has been observed for Co^{2+} substituted samples. Due to Co^{2+} substitution in crystallographic site the peak positions are shifted to the right side of $BaFe_{12}O_{19}$ sample. The results of XRD show that the strength of the peaks of $CoFe_2O_4$ phase increases as the doped Co^{2+} ion substitution increased. The similar results were found in literature for Co substituted $BaFe_{12}O_{19}$ and $SrFe_{12}O_{19}$ samples [10, 11]. To analyze the grain sizes and its distributions of the synthesized nano powders, their SEM images for the typical composition (x = 0.0 and 1.0) of Co^{2+} ions in $Ba_{1-x}Co_xFe_{12}O_{19}$ is presented in Figure 2. As can be seen from this figure, the distribution of particle size is almost homogeneous and the average particle sizes are below 100 nm for all of the samples.

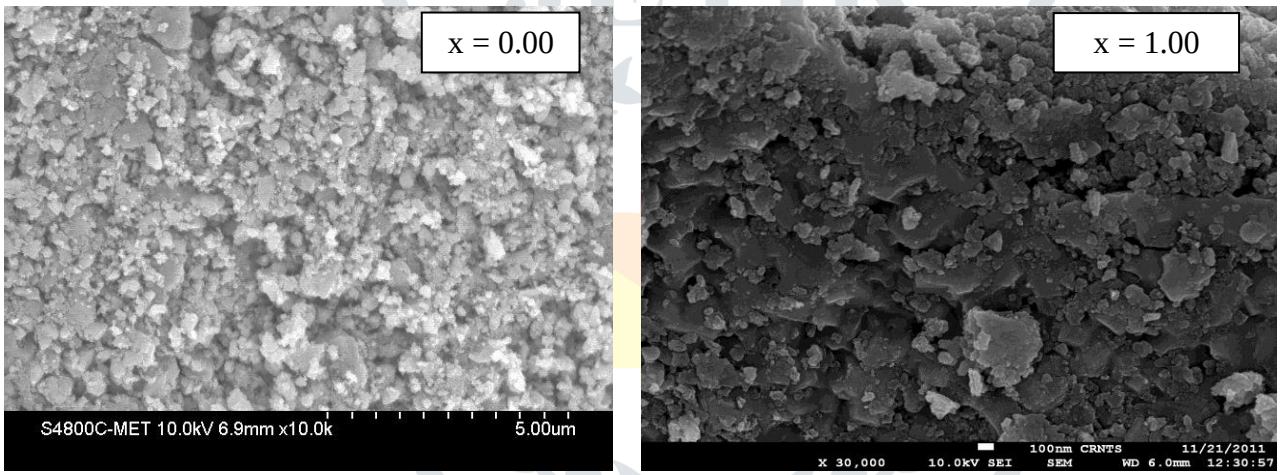

Fig. 2: SEM micrographs of $Ba_{1-x}Co_xFe_{12}O_{19}$

3.2 Diffuse Reflectance Spectroscopy

The band-gap energy and the optical property of the as-prepared material were measured by using an UV-Visible diffuse reflectance spectrometer at room temperature in the wavelength range of 200 to 800 nm. The optical absorption of the $Ba_{1-x}Co_xFe_{12}O_{19}$ (x= 0.0 to 1.00) ferrite nanoparticles is important due to the UV–vis absorption edge which is related to the band gap energy of the photocatalyst. Figures 3 and 4 shows the variation of optical absorption and transmittance spectra with wavelength respectively.

The band gap energy has been calculated from the spectrum from following relation

$$E = \frac{hc}{\lambda} \qquad (1)$$

$$E = \frac{6.625 \times 10^{-34} \times 3 \times 10^{8}}{\lambda_0} (eV) \quad (2)$$

where E is Band Gap energy, h is Planck's constant, λ_0 is Wavelength of first sharp peak from graph, c is velocity of light.

The band gap values concluded from graph are in the range of 2.322 eV to 3.26 eV. The value of band gap for pure barium hexaferrite is in the range of reported literature value of 2.32 [12]. The variation of band gap energy with Co^{2+} substitution x is depicted in Fig. 5. The graph shows that with substitution the band gap increases. The increase in the band gap value is attributed to the quantum confinement phenomenon taking place at the nano-regime. Quantum confinement at nanoscale plays important role in increasing the band gap.

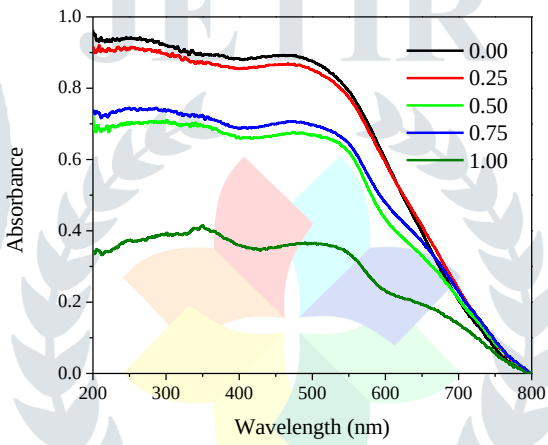

Fig. 3: Optical absorption with frequency for $Ba_{1-x}Co_xFe_{12}O_{19}$

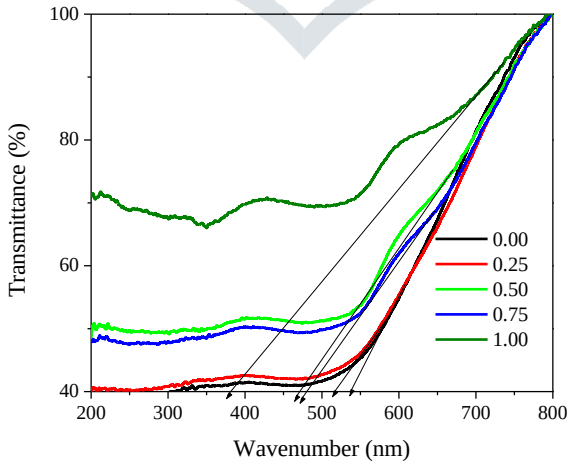

Fig. 4: Optical transmittance with frequency for $Ba_{1-x}Co_xFe_{12}O_{19}$

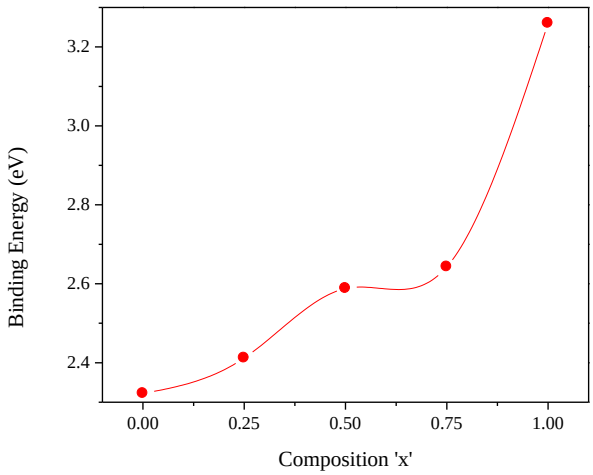

Fig. 5: Band gap energy of $Ba_{1-x}Co_xFe_{12}O_{19}$ (x= 0.0 to 1.00) nanoparticles

3.3 Electrical Properties

3.3.1 DC electrical resistivity

Figure 6 shows the variation of DC resistivity with the Co^{2+} ion substitution for $Ba_{1-x}Co_xFe_{12}O_{19}$. The DC electrical resistivity decreased with increase in temperature, this behavior confirmed the semiconducting nature of the prepared samples. In ferrites, the resistivity ρ is given by the relation

$$\rho = \rho_0 \exp\left(\frac{\Delta E}{kT}\right) \quad (3)$$

where ρ is the d.c. electrical resistivity at temperature T, ρ_0 is the pre-exponential factor with the dimensions of Ω-cm, k is the Boltzmann constant (8.6173439×10^{-5} eV/K), ΔE is the activation energy, and T is the absolute temperature.

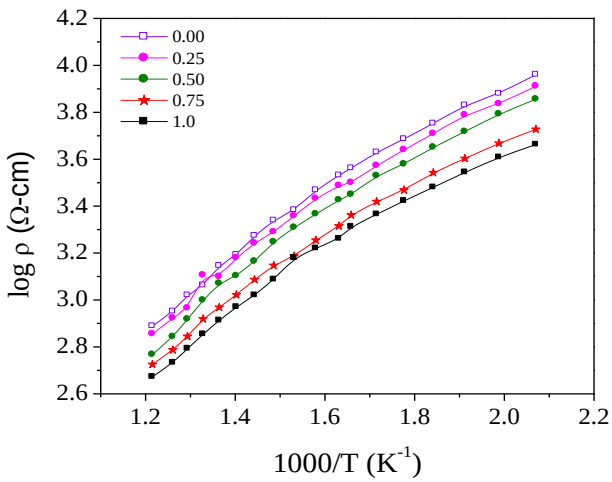

Fig. 6: Variation of logarithm of resistivity with reciprocal of logarithm of temperature for $Ba_{1-x}Co_xFe_{12}O_{19}$

In polycrystalline ferrite, cations are surrounded by close-packed oxygen anions and can well be treated as isolated from each other to a first approximation. The electrical conduction in ferrites can be explained by the Verwey model [13] of electron hopping, which involves the exchange of electrons between ions of the same element present in different valance states and distributed randomly over crystallographically equivalent lattice sites.

In the present system, the conduction is attributed to the exchange of 3d electrons between Fe^{2+} and Fe^{3+} ions. A small amount of Fe^{3+} is converted in to Fe^{2+} during sintering at high temperature. Figures 6 and 7 shows the observed decrease in resistivity can be understood by considering the hopping mechanism

$$Fe^{2+} \leftrightarrow Fe^{3+}$$

The substitution of Co^{2+} in the series may also make the following conduction mechanism possible [14, 15]:

$$Co^{2+}Fe^{3+} \leftrightarrow Co^{3+}Fe^{3+}.$$

The increase in Co^{2+} ions replaces Ba ions, decreasing the number of Ba ions formed, thereby causing an increase of the hopping between $Co^{2+}Fe^{3+} \leftrightarrow Co^{3+}Fe^{3+}$.

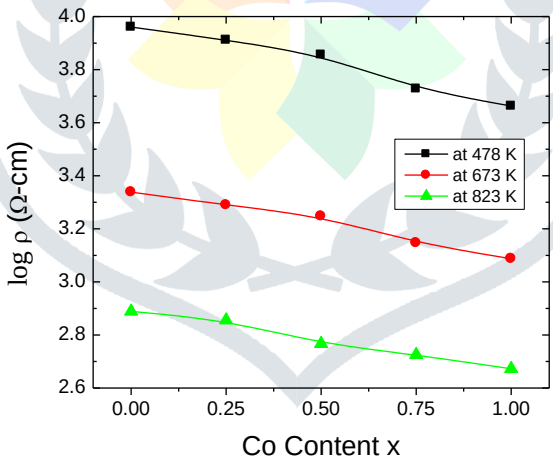

Fig. 7: Variation of logarithm resistivity with Co substitution for THREE selected temperature for $Ba_{1-x}Co_xFe_{12}O_{19}$

Dielectric properties

The value of real dielectric constant (ε′) has been calculated using the following relation:

$$\varepsilon' = \frac{Cp \times t}{\varepsilon_0 A} \qquad (4)$$

where $\varepsilon_0 = 8.85\times10^{-14}$ F/cm, known as permittivity of the free space t is the thickness of pellets, A is the cross sectional area of the flat surface of the pellets and Cp is the capacitance of the pellet in (F). The frequency dependence of dielectric constant from 100 Hz-6MHz, at room temperature is illustrated in Fig. 8.

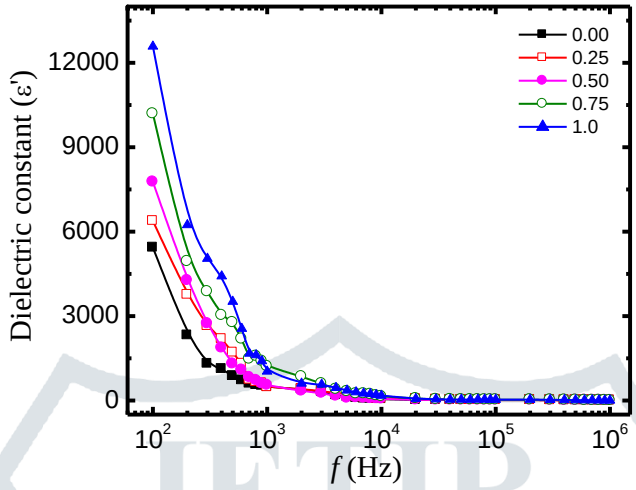

Fig. 8: Variation of dielectric constant with applied frequency for $Ba_{1-x}Co_xFe_{12}O_{19}$

It can be seen that all the samples revealed almost normal behavior, i.e. dielectric constant decreases rapidly initially with increase in frequency and reaches a constant value at higher frequency. The dielectric constant decrease rapidly in low frequency region and becomes almost frequency independent in high frequency region. This variation can be explained in terms of space charge polarization which is produced due to the presence of higher conductivity phases (grains) in the insulating matrix (grain boundaries) of a dielectric produces localized accumulation of charge under the influence of an electric field. The assembly of space charge carriers in a dielectric takes a finite time to line up their axes parallel to an alternating electric field. If the frequency of the field reversal increases, a point is reached where the space charge carriers cannot keep up with the field and the alternation of their direction lags behind that of the field. This results in a reduction of dielectric constant of the material. According to Maxwell and Wagner two-layer model [16-18] space charge polarization is because of inhomogeneous dielectric structure of the material. It is formed by large well conducting grains separated by thin poorly conducting intermediate grain boundaries. The transport of charge carrier creates the space charge polarization and these charge carriers are stopped at a potential barrier, which is possibly the grain boundary. This can also be understood by a mechanism similar to conduction mechanism. The electrical conduction in ferrite is explained by the Verwey mechanism of electron

hopping [19]. The electrons, by hopping, reach the grain boundary and due to its higher resistivity, the electrons get piled up, thereby producing space charge polarization.

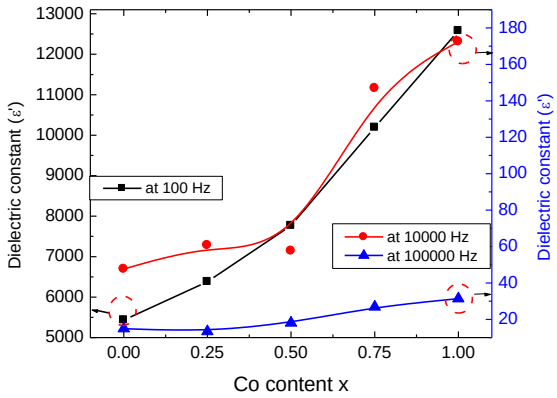

Fig. 9: Variation dielectric constant with Co substitution for THREE selected frequency for $Ba_{1-x}Co_xFe_{12}O_{19}$

In the present study, the substitution with Co^{2+} ions produces a change in the polarization so developed (Figs. 8 and 9). As Co^{2+} content is increased there is a decrease in Ba ions, However, the exchange process of $Ba^{2+} \leftrightarrow Ba^{3+}$ is weak compared to $Co^{2+} \leftrightarrow Co^{3+}$ and $Fe^{2+} \leftrightarrow Fe^{3+}$ hence $Fe^{2+} \leftrightarrow Fe^{3+}$ is assumed to be the dominant mechanism. The decrease in Ba ions increases the hopping motion of electrons. This in turn increases the piling up of electrons at the grain boundary, hence impeding the buildup of space charge polarization. Therefore, the value of dielectric constant increased with increase in Co^{2+} substitution.

Dielectric loss is an important part of the total core loss in ferrites [20]. The loss tangent has been calculated from the following relation:

$$\tan\delta = \frac{1}{2\pi f \varepsilon_0 \varepsilon' \rho} \qquad (5)$$

Fig. 10 shows the variation of dielectric loss tangent (tanδ) with frequency at room temperature. The loss tangent shows a normal behavior with frequency and decreases as the frequency of applied field increases. The low loss values at higher frequencies show the potential applications of these materials in microwave devices. The behavior of tanδ can be explained on the basis that in low frequency region, which corresponds to high resistivity (due to grain boundary), more energy is required for electron exchange between $Co^{2+} \leftrightarrow Co^{3+}$ and $Fe^{2+} \leftrightarrow Fe^{3+}$ ions, as a result the loss is high. In high frequency region, which corresponds to low resistivity (due to grains), small energy is required for electron transfer between $Co^{2+} \leftrightarrow$

Co^{3+} and $Fe^{2+} \leftrightarrow Fe^{3+}$ ions. Moreover, the dielectric loss factor also depends on number of factors, such as stoichiometry, Fe^{2+} content and structural homogeneity, which in turn, depend upon the composition and sintering temperature of the samples [21,22].

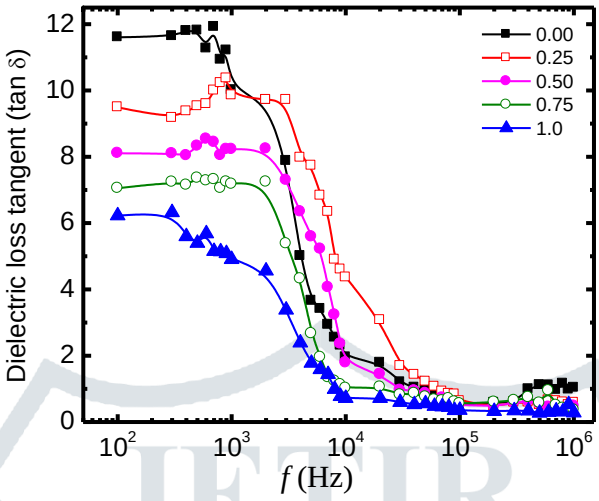

Fig. 10:Variation of dielectric loss tangent (tanδ) with applied frequency for $Ba_{1-x}Co_xFe_{12}O_{19}$

4. Conclusions

A series of divalent Co^{2+} substituted $BaFe_{12}O_{19}$ with a chemical formula $Ba_{1-x}Co_xFe_{12}O_{19}$ (x= 0.0, 0.25, 0.50, 0.75 and 1.0) were successfully prepared by sol-gel auto-combustion technique. X-ray diffraction investigations performed at room temperature shows formation of single phase hexagonal structure for undoped BaM and indicates influence of Co^{2+} substitution on the structure of material. The increase in the band gap value is attributed to the quantum confinement phenomenon taking place at the nano-regime. DC electrical resistivity decreased with the increase in temperature. This confirmed the semi-conducting behavior of Co^{2+} substituted $BaFe_{12}O_{19}$. Co^{2+} ions decrease the DC electrical resistivity due to the increase in hopping probability between Co^{2+} and Fe ions. Samples show normal ferrite dielectric behavior. Also, incorporation of Co^{2+} ion enhances dielectric response of BaM nanoparticles. The dielectric behavior obeys the Maxwell-Wagner polarization in accordance with Koops phenomenological theory.

References:

[1] Y. Naito, K. Suetake, IEEE Trans, Microwave Theor. Tech. MTT-19 (1971) 65–72.

[2] K. Ishino, Y. Narumity, Am. Ceram. Soc. Bull. 66 (1987) 1469–1474.

[3] J.Y. Shin, J.H. Oh, IEEE Trans. Magn. 29 (1993) 3437–3439.

[4] Xin Tang, Yuanguang Yang, Keao Hu, Structure and electromagnetic behavior of $BaFe_{12-2x}(Ni_{0.8}Ti_{0.7})_xO_{19-0.8x}$ in the 2–12GHz frequency range, J. Alloy. Compd. 477 (2009) 488–492

[5] S. Dixon, M. Weiner, T.R.A. Coin, Journal of Applied Physics 41 (1970) 1357.

[6] S. Sugimoto, K.Okayama, H.Ota, M. Kimura,Y. Yoshida, H. Nakamura, D. Book, T. Kagotani, M. Homma,J. Mag. Soc. Japan 23 (1999) 611.

[7] R. Carey, P. A. Gago-Sandval, D. M. Newman and B. W. J. Thomas, The magnetic and magneto-optical properties of Co, Cr, Mn and Ni substituted barium ferrite films, J. App. Phys.75 (1991) 6789-6791

[8] X. Batlle, X. Obradors, J. Rodríguez-Carvajal, M. Pernet, M. V. Cabañas and M. Vallet, Cation distribution and intrinsic magnetic properties of Co-Ti-doped M-type barium ferrite, J. App. Phys.70 (1991) 1614

[9] X. Batlle, M. García del Muro, J. Tejada, H. Pfeiffer, P. Görnert and E. Sinn, Magnetic study of M-type doped barium ferrite nanocrystalline powders, J. App. Phys. 74 (1993) 3333

[10] Darja Lisjak, Giovanni Bolelli, Luca Lusvarghi, Marion Begard, Markus Bruehl, Kirsten Bobzin, Pertti Lintunen, Ulla Kanerva, Massimo Pasquale, Miha Drofenik, Magnetic Phase Formation in CoTi-Substituted Ba Hexaferrite Coatings Prepared with Atmospheric Plasma Spraying, J. Amer. Ceram. Soci. 93 [9] (2010) 2579-2584

[11] S.E. Mousavi Ghahfarokhi, F.Ranjbar, M.Zargar Shoushtari, A study of the properties of $SrFe_{12-x}Co_xO_{19}$ nanoparticles, J. Magn. Magn. Mater. 349 (2014) 80-87

[12] S. Anjum, M. Shahid Rafique, M. Khaleeq-ur-Rahman, K. Siraj, A. Usman, I. Hussain, S. Naseem, Investigation of induced parallel magnetic anisotropy at low deposition temperature in Ba-hexaferrites thin films, J. Magn. Magn. Mater.324 (2012) 711-716

[13] E. J. Verwey, J. H. de Boer, Rec. Trav. Chim. Phys. Bas. 55 (1936) 531

[14] R.H. Kadam, Suresh T. Alone, Maheshkumar L. Mane, A.R. Biradar, Sagar E. Shirsath, Phase evaluation of Li^+ substituted $CoFe_2O_4$ nanoparticles, their characterizations and magnetic properties, J. Magn. Magn. Mater. 355 (2014) 70–75

[15] Mohd. Hashim, S.S. Meena, R.K. Kotnala, Sagar E. Shirsath, Pramod Bhatt, Shalendra Kumar, Erdoğan Şentürk, Ravi Kumar, Nidhi Gupta, Alimuddin, Exploring the structural, Mössbauer and dielectric properties of Co^{2+} incorporated $Mg_{0.5}Zn_{0.5-x}Co_xFe_2O_4$ nanocrystalline ferrite, J. Magn. Magn. Mater. 360(2014)21-33.

[16] C.G. Koops, On the dispersion of resistivity and dielectric constant of some semiconductors at audio frequencies, Physical Review 83 (1951) 121-124

[17] J.C. Maxwell, Electricity and Magnetism, vol. 1, Oxford University Press, London, 1954 section 328

[18] K.W. Wagner, Zur theorie der unvoll Kommener dielektrika, Ann. Phys. (Germany) 40 (1913) 817-855

[19] E.J.W. Verwey, P.W. Haayman, F.C. Romeijn, Physical properties and cation arrangement of oxides with spinel structures, II: Electronic conductivity, Journal of Chemical Physics 15 (1947) 181-187

[20] J. Zhu, K.J. Tseng, C.F. Foo, Effects of multi-segment structure in core loss reduction of MnZn ferrite at high frequencies, IEEE Trans. Magnet. 36 (2000) 3408-3410

[21] S. S. Bellad, B. K. Chougle, Composition and frequency dependent dielectric properties of Li–Mg–Ti ferrites, Materials Chemistry and Physics, 66 (2000) 58

[22] Sagar E. Shirsath, B.G. Toksha, Maheshkumar L. Mane, V.N. Dhage, D.R. Shengule, K.M. Jadhav, Frequency, temperature and In^{3+} dependent electrical conduction in $NiFe_2O_4$ powder, Powder Technology 212 (2011) 218–223.